

## Correlation between Fiber Density Distribution and Flexural Capacity of SFRC Beams Using Optical Density Analysis of X-ray Image

JSCE Student Member Sopokhem Lim, Waseda University  
 JSCE Student Member, Takehiro Okamoto, Waseda University  
 JSCE Member, Mitsuyoshi Akiyama, Waseda University  
 JSCE Member, Atsushi Koizumi, Waseda University

### 1. INTRODUCTION

De Montagnac et al. (2012) concluded discrepancies of their predicting model, often overestimated flexural strength of SFRC structural beams, were mainly due to dispersion of material properties and the differences of steel fiber orientation between beams and characterization specimens. To create a reliable prediction, Robins et al. (2003) and (2006) used X-ray images of some sliced small-scale specimens to obtain steel fiber distribution properties. These properties were used for forming a general tensile stress profile to combine with a single pull-out fiber test result and for estimating the flexural strength of SFRC beams. The present study investigates a statistic correlation between fiber distribution data analysis of X-ray images and flexural capacity of specimens. The result of this correlation proves the validity of using X-ray images to formulate a numerical model for estimating the flexural strength of SFRC members.

### 2. EXPERIMENTAL PROGRAM

Two series of SFRC beams (1460mm x 140mm x 80mm) were established, each of which consisted of two specimens with identical properties. The used steel fiber (5D65/60BG) was 60mm long with diameter of 0.9mm. Two volume fractions of fiber 0.5% and 1.1% were used in the mixing to investigate the effect of fiber amount on flexural behavior of the beams. The specimens were cured before the four-point bending test at the age of 28 days. During the curing period, each specimen was taken using X-ray configuration shown in Fig. 1 to capture steel fiber distribution in the constant-moment region. The details of beam bending test setup and locations of X-ray photography are shown in Fig.2. Table 1 shows the details of specimens.

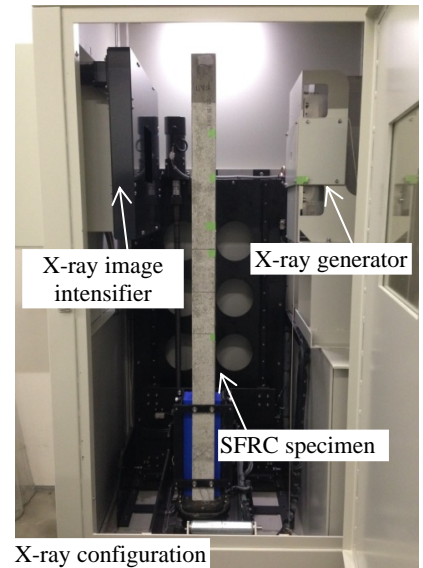


Fig. 1 X-ray configuration

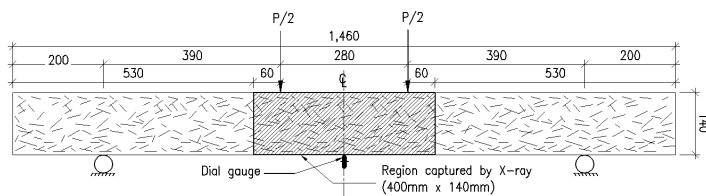


Fig.2 Details of beam bending test setup

Table.1 Details of Specimens

Notation	#	Section (mm)	% $V_f$	Fiber Shape
FB05	2	140x80	0.5%	
FB11	2	140x80	1.1%	

### 3. OPTICAL DENSITY (OD) ANALYSIS AND PROFILE LINE

OD analysis is an image processing application used to determine the amount of matters or objects in material by measuring the amount of light passing through it. During X-ray test, X-ray radiation penetrates through a SFRC specimen visualizing and creating a grey scale image of steel fibers distributed inside the concrete composite. When magnified as in Photo.1, the obtained image shows steel fibers produce tiny elements on the image called pixels which have darker levels or higher OD than the composite because the former have higher density than the latter. Arrayed in grids by row  $x$  and column  $y$  numbers, the dark and bright pixels or so-called intensity have represented index values ranging from 0 to 255, 0 for pure black and 255 for pure white. OD values have an inversed relationship with the values of pixel or intensity by formula:

$$OD(x, y) = -\log \left[ \frac{\text{intensity}(x, y) - \text{black}}{\text{incident} - \text{black}} \right] \quad (1)$$

where  $\text{intensity}(x, y)$  is the intensity at  $\text{pixel}(x, y)$ ,  $\text{black}$  is the intensity generated when no light goes through the material,

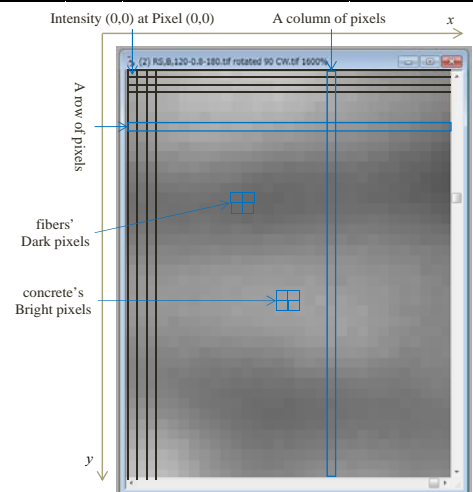


Photo 1 X-ray image zoomed in 1600%

Keywords: SFRC, X-ray, Steel fiber distribution

Contact address: Bldg. 51-16-09, Oukubo 3-4-1, Shinjuku-ku, Tokyo, 169-8555, Japan, Tel: +81-3-5286-2694

and *Incident* is the intensity obtained when no object is in between the camera's lens and radiation source. The averaged values of the accumulated OD in each column numbers of pixels (hereinafter referring to as  $\zeta$ ) can be estimated by the formula:

$$\zeta(y) = \frac{\sum_{x=1}^k OD(x, y)}{k} \quad (2)$$

where  $k$  is the number of rows of pixels and  $y=1, \dots, n$  in which  $n$  is the number of columns of pixels. Plotting these averaged values in  $y$ -axis against the length of the side beam in  $x$ -axis, a profile line illustrating steel fiber density distribution along the beam length captured by X-ray images can be obtained (see Fig. 3).

#### 4. RESULTS AND DISCUSSION

Fig. 3 shows a profile line of  $\zeta$  values between the upper and lower lines (BC) and (OA) of the connected X-ray images in Photo 2. It should be noted that the vertical dotted lines C1 to C6 in the graph are corresponded and therefore superimposed to the six joints of X-ray images respectively to make it easy for side-by-side comparison. The graph shows the values of  $\zeta$  fluctuating in between 0.32 and 0.64 ( $0.32 < \zeta < 0.64$ ) from the axis's origin to line C5 are mostly higher than those in between 0.30 and 0.44 ( $0.3 < \zeta < 0.44$ ) from line C5 and C6. This results from the fact that the density of steel fibers from lines OB to C5 is higher than that of fibers from lines C5 to C6 on the X-ray image. From line C6 up to the point of 342.92mm, the  $\zeta$  values are the set of lowest values comparing to the rest, indicating the least number of fibers present at the corresponding region on the X-ray image from lines C6 till the right edge of image. It is also interesting to note that the minimum value of  $\zeta$  indicates the location of the lowest density or number of steel fibers which, in turn, determines the location of critical section that causes a singly localized crack of the beam and governs flexural capacity of the specimen. On the other hand, the abrupt declines of  $\zeta$  values at each connected joints between X-ray images, lines C1 to C6 in Fig. 3, dictates that each connection of X-ray images contains errors. The connection errors also lead to the shortening of total length of connected X-ray images, 342.92mm long in Fig. 3 different from the real one 400mm long. These problems are mainly due to different fractional angles of X-ray radiation from a focal point of X-ray source, making objects appear on the image different from real-life ones. However, the correlation between minimum  $\zeta$  values obtained from single images of each beam and flexural loads plotted in Fig. 4 indicates a good relationship with  $R^2=0.96$ . This explains the data analysis on a single X-ray image without connection is proved validated for formulation of a numerical model to estimate the flexural capacity.

From line C6 up to the point of 342.92mm, the  $\zeta$  values are the set of lowest values comparing to the rest, indicating the least number of fibers present at the corresponding region on the X-ray image from lines C6 till the right edge of image. It is also interesting to note that the minimum value of  $\zeta$  indicates the location of the lowest density or number of steel fibers which, in turn, determines the location of critical section that causes a singly localized crack of the beam and governs flexural capacity of the specimen. On the other hand, the abrupt declines of  $\zeta$  values at each connected joints between X-ray images, lines C1 to C6 in Fig. 3, dictates that each connection of X-ray images contains errors. The connection errors also lead to the shortening of total length of connected X-ray images, 342.92mm long in Fig. 3 different from the real one 400mm long. These problems are mainly due to different fractional angles of X-ray radiation from a focal point of X-ray source, making objects appear on the image different from real-life ones. However, the correlation between minimum  $\zeta$  values obtained from single images of each beam and flexural loads plotted in Fig. 4 indicates a good relationship with  $R^2=0.96$ . This explains the data analysis on a single X-ray image without connection is proved validated for formulation of a numerical model to estimate the flexural capacity.

#### 5. CONCLUSIONS

The statistic data analysis of OD of connected X-ray images can be used to plot a profile line of fiber density distribution along the length of specimens. The minimum value of the profile line can be used to predict location of critical cross section of the specimen at which a single onset crack occurs. Moreover, a good correlation between minimum  $\zeta$  values and flexural loads with  $R^2=0.96$  proved information of X-ray images of every specimen are validated to establish a numerical method to estimate the flexural capacity of SFRC beam.

**ACKNOWLEDGEMENT** The authors express sincere appreciation to Mr. Gan Cheng Chian at BEKAERT Singapore Pte Ltd. and Dr. Hexiang Dong at BEKAERT Japan Co., Ltd. for their kind supports and cooperations for this experiment. The options and conclusions presented in this paper are those of the authors and do not reflect the views of the sponsoring organizations.

#### REFERENCES

- DE Montaignac, R., Massicotte, B., Charron, J-P.: Design of SFRC Structural Elements: Flexural Behavior Prediction, Materials and Structures, 45, 2012, pp. 623-636.
- Robins, P. J., Austin S. A., Jones P. A.: Spatial Distribution of Steel Fibres in Sprayed and Cast Concrete, Magazine of Concrete Research, 55-3, 2003, pp. 225-235.
- Robins, P. J., Austin S. A., Jones P. A.: Predicting the Flexural Load-Deflection Response of Steel Fibre Reinforced Concrete from Strain, Crack-Width, Fibre Pull-Out and Distribution Data, Materials and Structures, 2008, 41, pp. 449-463.

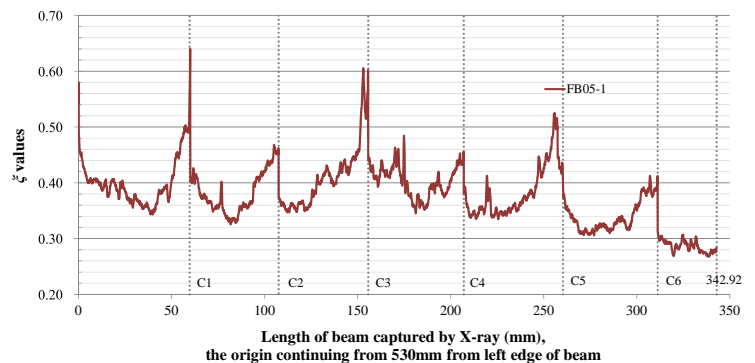
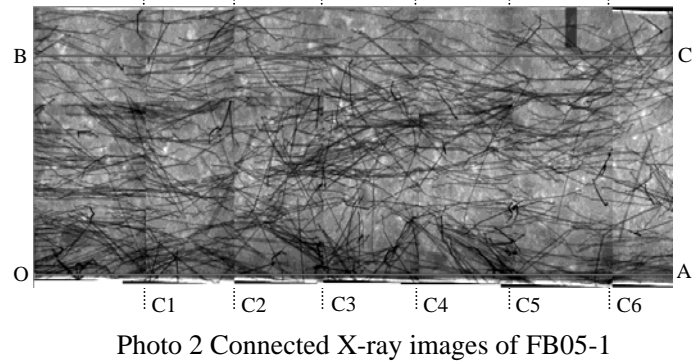


Fig. 3 Profile lines of  $\zeta$  values at region captured by X-ray

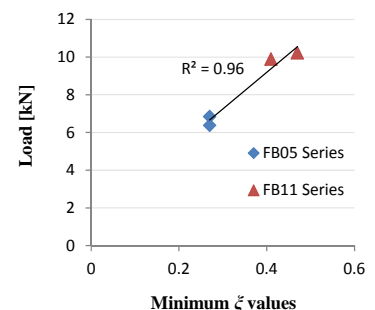


Fig. 4 Correlation between min.  $\zeta$  values and flexural loads